Journal of Materials Chemistry C

Accepted Manuscript

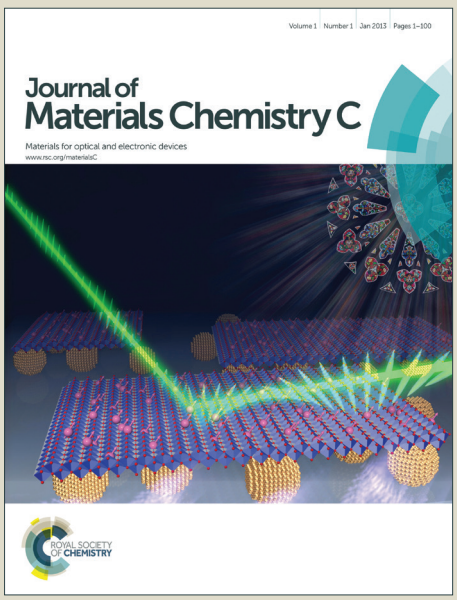

ROYAL SOCIETY OF CHEMISTRY

www.rsc.org/materialsC

Journal of Materials Chemistry C

Cite this: DOI: 10.1039/c0xx00000x

www.rsc.org/xxxxxx

ARTICLE TYPE

Synthesis and characterization of arylamino end-capped sliafluorenes for blue to deep-blue organic light-emitting diodes (OLEDs) †

Shao Fu Chen[a], Yuan Tian[b], Jinghong Peng[b], Huarong Zhang[a], Xin Jiang Feng*[a], Haixia Zhang[a], Xinjun Xu*[b], Lidong Li[b], Jianhua Gao[a]

Received (in XXX, XXX) Xth XXXXXXXXX 20XX, Accepted Xth XXXXXXXXX 20XX
DOI: 10.1039/b000000x

Diphenylamino- or cabazolyl-endcapped silafluorene derivatives which show a wide energy band gap, a high fluorescence quantum yield and high stability have been designed, synthesized, and characterized. Double-layer electroluminescent devices of these silafluorene derivatives exhibited efficient blue emission. The non-doped double-layer OLEDs containing **TDMS**, **TDPS**, **CDMS**, or **CDPS** exhibited better electroluminescence (EL) efficiencies than those of the devices using the reference emitter **DPFL-NPB**, among which the best device with **TDPS** showed a maximum current efficiency of 1.62 cd/A and an external quantum efficiency (EQE) of 1.36%. The solution processed device using **TDPS** as dopant exhibited high performance with an EQE of 2.48% and an obviously low turn-on voltage of 4 V, as compared to those of the reference device. The replacement of carbon atom of fluorene unit with silicon atom can lower the energy gap effectively and improve thermal stability as well as optical performances. The results indicate that the end-capped arylamino groups affect the OLED performances greatly and aryl or alkyl substitution on 9-position of silafluorene unit is also crucial to the OLED performances of this kind of silafluorenes.

Introduction

The development of materials and device engineering in organic light-emitting diodes (OLEDs) realized the practical applications in OLED displays and solid-state lightings [1-6]. However, blue-emitting materials and devices are still needed to be improved regarding to efficiency, lifetime and color purity as compared to those of green and red emitters and devices. Up to date, blue OLEDs with high external quantum efficiecy (EQE) are still limited, because these materials require a high fluorescence yield, a wide energy band gap, a high thermal stability and good thin film morphology [7-12]. As a result, developing blue emitters for OLED applications still remains a challenge [13].

Fluorene derivatives are widely used as OLED materials over the past decades [14-25]. However, long wavelength emission, derived from excimer emission and/or the oxidation of the 9-position on fluorene ring, is a deadly disadvantage for this kind of materials to serve as blue emission materials in OLEDs [26, 27]. To overcome the disadvantages from the latter, silafluorene derivatives have been explored to replace the corresponding fluorene derivatives and exhibited promising properties [28-29]. Furthermore, introduction of arylamino groups, such as diphenylamino- or cabazolyl, are common methods for design of OLED materials [30-34].

The aim of the present work is to study the series of fluorescent arylamino end-capped silafluorene derivatives in which the photonic and electronic properties are systematically varied by chemical modification with different substituent groups on silicon atom and end-capped arylamino groups. To exploit them as emitters in OLEDs, sublimated double-layer devices using **TDMS**, **TDPS**, **CDMS**, and **CDPS** (Scheme 1) as emitting-layer were fabricated to evaluate their electroluminescent properties by comparison with a commercially available material, **DPFL-NPB** (9*H*-Fluorene-2,7-diamine, N^2,N^7-di-1-naphthalenyl-N^2,N^7,9,9-tetraphenyl-), among which the device with **TDPS** exhibits the best performances in the blue region with CIE coordinates of (0.175, 0.144). Further optimization by adding electron-transporting/hole-blocking in different layers, the solution processed devices exhibit enhanced EL performances. The best device with **TDPS** exhibited a maximum luminance of 5501cd/m^2, an external quantum yield of 2.48%, a maximum luminous efficiency of 2.81cd/A and a low turn-on voltage of 4V.

Results and discussion

Synthesis

The molecular structures of the blue-emitting silafluorene derivatives and their synthetic routes are outlined in Scheme 1. Intermediate 4 was prepared from 2,5-dibromonitrobenzene according to the literature[35]. The target compounds were prepared by Palladium catalyzed Suzuki cross-coupling reaction of (4-(diphenylamino)phenyl)boronic acid, 7 or (4-(9H-carbazol-9-yl)phenyl)boronic acid, 8 with the corresponding silafluorene derivatives 5 and 6. The yields are 69%, 68%, 34%, and 45% for **TDMS**, **TDPS**, **CDMS**, and **CDPS**, respectively. All the

molecules were fully characterized by NMR spectroscopy, elemental analysis, and high-resolution mass spectrometry and found to be in good agreement with the structures.

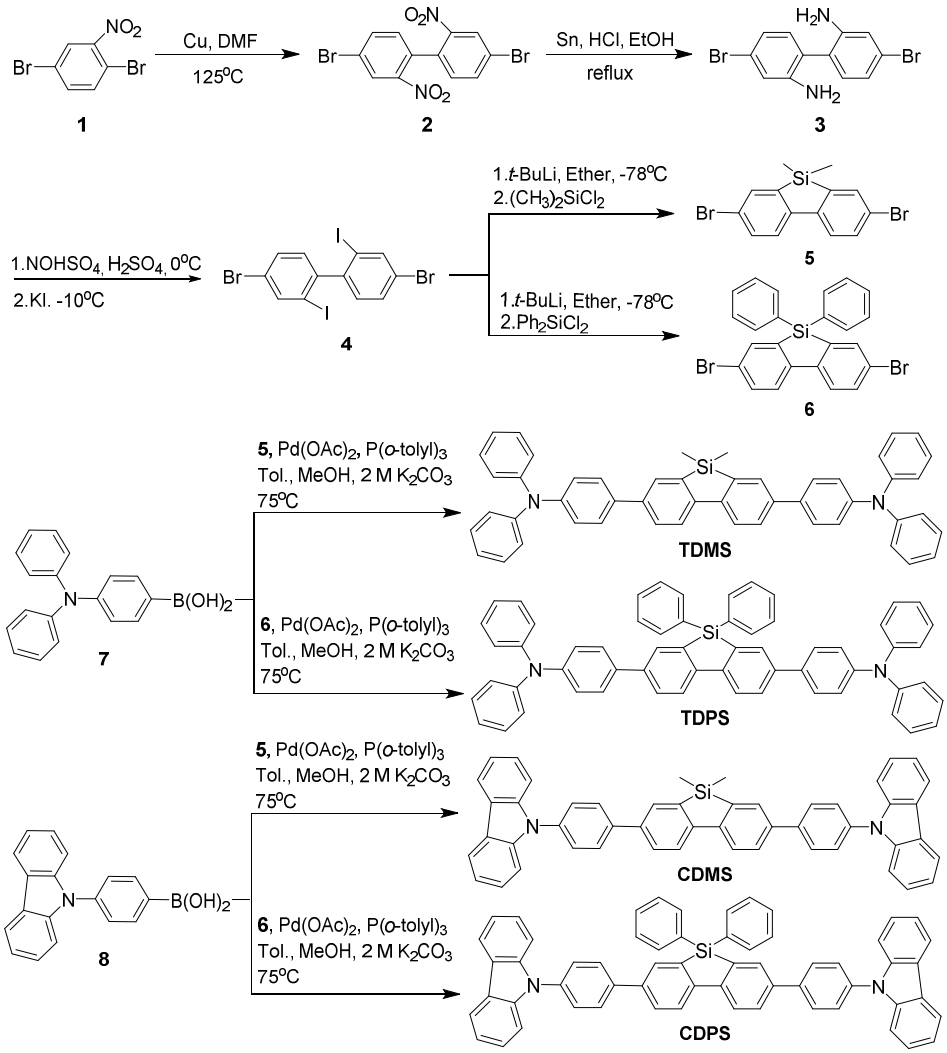

Scheme 1 Synthesis of silafluorenes.

Photophysical, electrochemical, and thermal properties

The photophysical, electrochemical, and thermal properties of these silafluorenes are summarized in Table 1 and Table 2. Figure 1a, 1b, and 1c show the absorption and emission characteristics of these materials in toluene, chloroform, and DMF, respectively. All the derivatives show similar absorption spectral features, which are composed of two major absorption bands. The stronger absorption peaks span from 344-378 nm corresponding to the π→π* transition of the π-conjugated cores and the weaker absorption peaks appear around 300 nm due to the n→π* transition of arylamino moieties. In general, the carbazolyl end-capped derivarives exhibit blue-shifted spectra in both absorption and emission as compared with the diphenylamino substituted ones, because the carbazolyl is a weaker electron donor than the diphenylamino group and molecules end-capped with carbazolyl are of more coplanarity. Upon excitation at the absorption maximum, these silafluorene derivatives exhibit strong blue fluorescence with peaks ranging from 394 nm to 462 nm in solution and from 410 nm to 436 nm in thin film. Red-shifts of 14 nm to 21 nm are observed for the emission maxima in thin film compared to those in toluene, indicating the aggregation of molecules in the solid state. Solvatochromism effects are observed for these materials. For instance, the emission maxima of **TDMS** exhibit solvatochromic shift of 11 nm and 22 nm changing from toluene to chloroform and from chloroform to DMF, respectively, which indicates the intramolecular charge transfer (ICT) properties of these oligomers (see Figure 1d). The fluorescence quantum yields measured in solution are high in the range of 0.57-0.93, while the corresponding quantum yields for powder are 0.26, 0.22, 0.33, and 0.19 for **TDMS**, **TDPS**, **CDMS**, and **CDPS**, respectively (see Table 1), showing the potential for OLED applications of these materials.

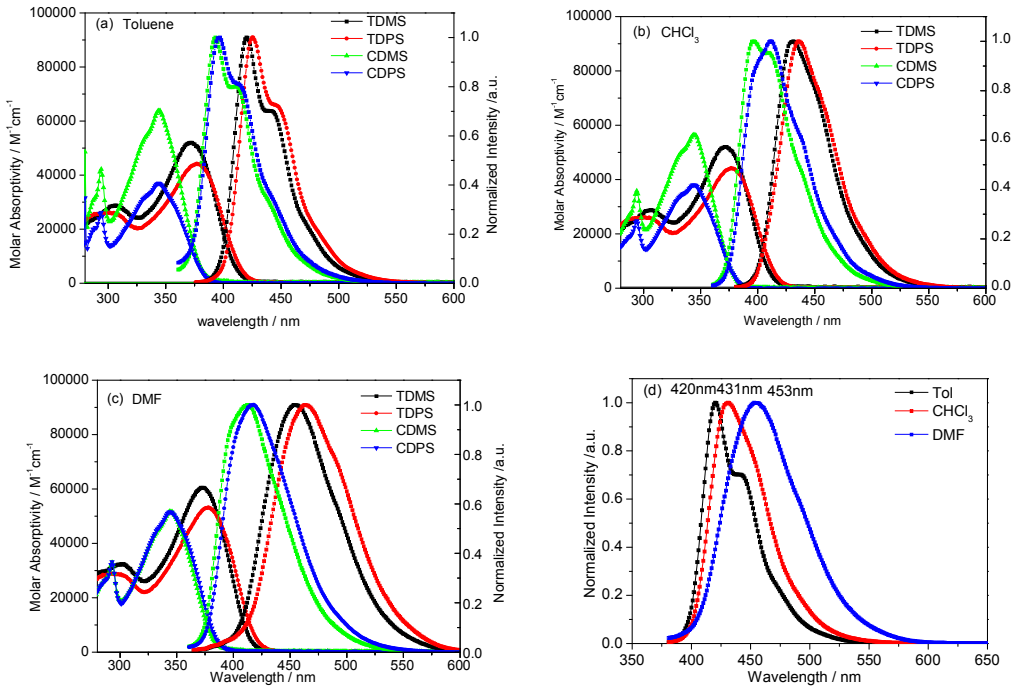

Fig.1 Absorption and emission of silafluorenes in toluene (a), chloroform (b), and DMF (c) and solvatochromic effect of **TDMS** (d).

Table 1 Photophysical properties of silafluorene derivatives

	λ^{abs}_{max} (nm)	λ^{em}_{max} (nm)[a]	Φ_{FL}	λ^{abs}_{max} (nm)	λ^{em}_{max} (nm)[a]	Φ_{FL}	λ^{abs}_{max} (nm)	λ^{em}_{max} (nm)[a]	Φ_{FL}	λ^{abs}_{max} (nm)	λ^{em}_{max} (nm)	Φ_{FL}
	Toluene			Chloroform			DMF			Powder		
TDMS	371	420	0.86[b]	371	431	0.74[b]	371	453	0.69[b]	382	436	0.26
TDPS	376	426	0.76[b]	378	436	0.87[b]	378	462	0.58[b]	389	440	0.22
CDMS	344	394	0.75[c]	345	397	0.76[c]	344	413	0.58[c]	363	415	0.33
CDPS	345	396	0.72[c]	344	400	0.93[c]	344	418	0.57[c]	363	410	0.19

[a]excited at the absorption maxima [b]using quinine sulfate monohydrate (Φ_{350} = 0.58) as a standard. [c]using quinine sulfate monohydrate (Φ_{313} = 0.48) as a standard.

Table 2 Electrochemical and thermal properties of silafluorene derivatives Caption

	E_{onset}^{oxd}[a] (V)	HOMO[b] (eV)	LUMO[c] (eV)	E_g^{opt}[d] (eV)	T_g[e] (°C)	T_m[e] (°C)	T_d[f] (°C)
TDMS	0.51	-5.22	-2.30	2.92	118	269	454
TDPS	0.48	-5.19	-2.34	2.85	-	290	490
CDMS	0.94	-5.65	-2.39	3.26	-	380	386
CDPS	0.89	-5.60	-2.42	3.18	142	383	474

[a]E_{onset} vs Fc^+/Fc estimated by CV method using platinum disc electrode as a working electrode, platinum wire as a counter electrode, and $Ag/AgNO_3$ as a reference electrode in dichloromethane using Bu_4NPF_6 (0.1 M) as a supporting electrolyte and all the potentials were calibrated with ferrocene. [b]calculated from CV measurements. [c]$E_g^{opt} = E_{LUMO} - E_{HOMO}$. [d]estimated by absorption cutoff. [e]determined by differential scanning calorimeter from re-melt after cooling with a heating rate of 10 °C/min under N_2. [f]determined by thermal gravimetric analyser with a heating rate of 20 °C/min under N_2.

To probe the redox properties of these arylamino end-capped silafluorenes, cyclic voltammetry (CV) was performed in dichloromethane using Bu_4NPF_6 (0.1 M) as a supporting electrolyte. All the molecules exhibit a reversible one-electron oxidation waves corresponding to the sequential removal of an electron from the triarylamine with E_{onset} of 0.51 V, 0.48 V, 0.94 V, and 0.89 V for **TDMS**, **TDPS**, **CDMS**, and **CDPS**, respectively (Figure S1, ESI†). By using equation 1 [36], their HOMO energies from onset of first oxidation potentials were estimated as -5.22 eV, -5.19 eV, -5.65 eV, and -5.60 eV for **TDMS**, **TDPS**, **CDMS**, and **CDPS**, respectively, assuming that the absolute energy level of Fc/Fc^+ redox couple to be 4.8 eV below vacuum. Ferrocence was used as an external standard (0.09 V *vs* Ag/Ag^+). The energy gaps, determined by absorption cutoff, were -2.92 eV, -2.85 eV, -3.26 eV and, -3.18 eV for **TDMS**, **TDPS**, **CDMS**, and **CDPS**, respectively. As a result, the LUMO of these molecules, calculated by E_g = HOMO-LUMO, are -2.30 eV, -2.34 eV, -2.39 eV, and -2.42 eV for **TDMS**, **TDPS**, **CDMS**, and **CDPS**, respectively (see Table 2). The E_g of **TDMS** has an obvious decrease as compared with that of the corresponding fluorene derivative reported, [37] which manifests that energy gap could be lowered by introduction of silicon atom into 9-position of fluorene unit. The molecular orbital data indicate that the energy gaps of carbazolyl substituted derivatives are obviously high than those of the diphenylamino substituted ones, which are largely derived from the decrease of the corresponding HOMO levels of the carbazolyl substituted derivatives, while the decreases of LUMO levels affect slightly on the increase of the energy gaps. Nevertheless, slight decreases of HOMO and

LUMO levels still could be observed both in carbazolyl derivatives and diphenylamino derivatives when methyl groups were displaced by phenyl groups on 9-positon of the silafluorene units.

$$E_{HOMO} = -e(E_{onset(ox,dye)} - E_{onset(Fc)} + 4.8) \quad (1)$$

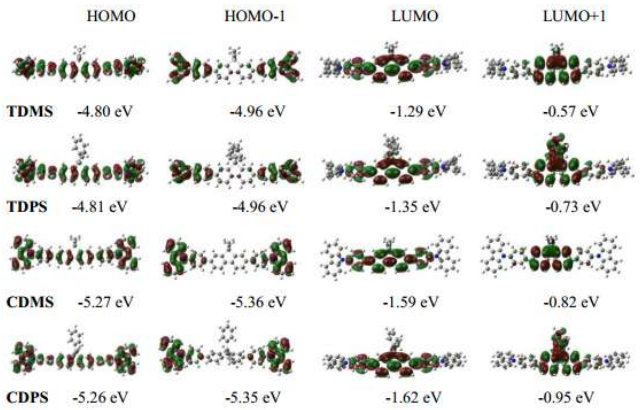

Fig. 2 Frontier molecular orbital diagrams and MO values of **TDMS**, **TDPS**, **CDMS**, and **CDPS**.

DFT (B3LYP, 6-31G (d,p)) calculations for molecular orbitals (MO) of the molecules have been performed by using Gaussian09 package [38]. Figure 2 illustrates the frontier molecular orbitals (HOMO, HOMO-1, LUMO and LUMO+1) and the corresponding values. The HOMOs of all the studied compounds are delocalized on throughout the backbone and electron donating groups. The LUMOs are localized on the backbones of the molecules. While the HOMO-1 and the LUMO+1 are more localized and mainly focused on the donating groups and conjugation cores as compared with HOMO and LUMO, respectively. The charge distribution in unoccupied MO reveals the intramolecular charge transfer in these molecules. The substituents on the silicon atom have no participation in the formation of HOMO and LUMO, which is also consistent with the emission spectra in solution of the materials that diphenyl-substituted derivatives **TDPS** and **CDPS** show no obvious red-shift in the emission spectra compared with the dimethyl-substituted ones, **TDMS** and **CDMS**, respectively. The resulting energy gaps calculated from HOMO and LUMO are 3.51 eV, 3.46 eV, 3.68 eV, and 3.64 eV for **TDMS**, **TDPS**, **CDMS**, and **CDPS**, respectively. The theoretical calculation reveals similar trend of energy changes in HOMO, LUMO, and E_g, as compared with those determined by CV and absorption cutoff, when changing the amino group at molecule terminals or substituents on 9-position of the silafluorene units.

The thermal properties of these silafluorenes were determined by differential scanning calorimetry (DSC) and thermogravimetric analysis (TGA) measurements (see Table 2). These silafluorenes exhibit high thermal stabilities with decomposition temperatures (T_d) higher than 386 °C. In addition, they exhibit high glass transition temperature (T_g) (Table 2). The high T_g and T_d values of these materials suggest stable morphological properties, which is desirable for OLEDs with high thermal stability.

The strong blue emission, good thermal stability, and relatively large energy gap (E_g) of these silafluorene derivatives imply that these compounds can be employed as potential blue emitters in OLED devices.

Electroluminescence performance

To investigate the EL performance of these materials, non-doped double-layer electroluminescent devices (as shown in Scheme 2, device A) have been fabricated with configuration of ITO/EML(50nm)/TPBi(20nm)/Ca/Al, where EML = **TDMS**, **TDPS**, **CDMS**, **CPDS**, and the reference material **DPFL-NPB**.

1,3,5-tris(*N*-phenylbenzimidazol-2-yl)benzene (TPBi) was used as a hole-blocking layer. Figure 3 depicts the normalized electroluminescence (EL) spectra of the non-doped double-layer OLEDs (Device A). The EL maxima peaked at 458nm and 464nm are in the deep-blue to blue range for the devices of **TDMS** and **TDPS**, respectively. The narrow full width half maximum (FWHM, 60nm and 66nm for **TDMS** and **TDPS**, respectively and CIE*x*,*y* (Commission Internationale de l'Eclairage, (0.156, 0.100) for **TDMS** and (0.175, 0.144) for **TDPS**) of these two devices also indicate that devices with **TDMS** and **TDPS** exhibit better color purity than those of the devices with **CDMS** and **CDPS**. However, the EL spectra of devices using **TDPS**, **CDMS** and **CDPS** as EML became broad to some extent and exhibit long wavelength emission, which maybe derives from the excimer emission in these devices (Figure 3 and Table 3).

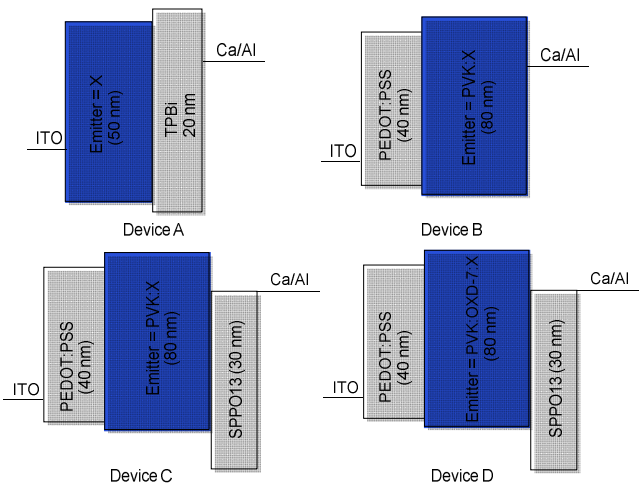

Scheme 2 Diagram of the device configurations.

Detailed EL performances of all devices are summarized in Table 3 and figure 4. First of all, double-layer devices with silafluorene emitters have significant better performances in luminance, current efficiency, power efficiency, and external quantum efficiency than those of the device with the reference material as EML. The efficiencies of the device using **TPDS** as EML are the best. The maximum luminance, current efficiency, power efficiency, and external quantum efficiency are 1.62cd/A, 0.38lm/W, 1792cd/m^2, and 1.36%, respectively. All these values are several times as high as those of the reference device. Meanwhile, the voltages at a current density of 20mA/cm^2 are comparable to that of the reference device, which could also be

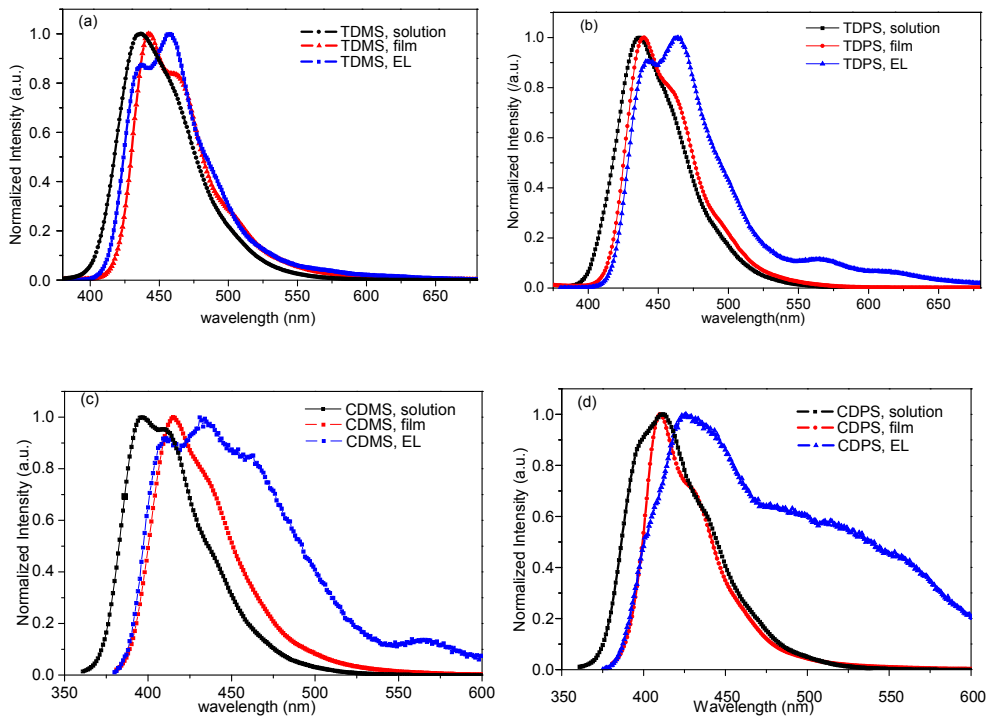

Fig. 3 PL spectra of silafluorenes in chloroform, film and EL spectra of **TDMS**, **TPMS**, **CDMS**, and **CPMS**.

Table 3 Summary of EL device performance of silafluorene derivatives based on device A

Device	V_{on} [a] (V)	V_{20} [b] (V)	$\eta_{l,20}$ [c] (cd/A)	$\eta_{l,max}$ [d] (cd/A)	$\eta_{p,20}$ [e] (lm/W)	$\eta_{p,max}$ [f] (lm/W)	L_{20} [g] (cd/m^2)	L_{max} [h] (cd/m^2)	EQE[i] (%)	λ_{EL}(fwhm)[j] (nm)	CIE (x,y)
TDMS	6.0	10.8	0.51	1.06	0.15	0.23	101	1760	1.19	458(60)	0.156, 0.100
TDPS	7.4	14.4	1.61	1.62	0.35	0.38	328	1794	1.36	464(66)	0.175, 0.144
CDMS	13.6	20.0	1.27	1.28	0.20	0.20	271	801	1.32	431(95)	0.179, 0.136
CDPS	8.4	14.4	0.65	0.74	0.14	0.14	139	2151	0.39	441(166)	0.264, 0.279
DPFL-NPB	5.2	13.2	0.59	0.59	0.14	0.15	116	375	0.41	465(78)	0.167, 0.188

[a] Turn on voltage when a brightness of 1 cd/m^2 observed. [b]Voltage taken at a current density of 20 mA/cm^2. [c]Current efficiency at a current density of 20 mA/cm^2. [d]Maximun current efficiency [e]Power efficiency at a current density of 20 mA/cm^2. [f]Maximum power efficiency. [g]Luminance at a current density of 20 mA/cm^2. [h]Maximum Luminance [i]External quantum efficiency at a current density of 20 mA/cm^2. [j]Full-width at half-maximum.

observed from the J-V-L curves depicted in Figure 4. Moreover, the good voltage-current density characteristics of the devices also indicates the good hole injection/transporting abilities of these materials. For example, the current densities of device with **TDMS** are obviously high than those of the reference device at the same voltage. As can be seen in the results, the diphenyl amino substituted derivatives exhibit superior device performances to the carbazolyl substituted ones, which is reasonable that the diphenyl amino substituted silafluorenes have lower E_g and the HOMOs fit ITO better as compared with the carbazolyl substituted ones (Figure 5). On the other hand, replacement of dimethyl groups by diphenyl ones on the 9-position of silafluorene also improves device performances.

The absorption spectra of **TDMS** and **TDPS** overlap well with the emission spectrum of PVK (polyvinylcarbazole) around 380 nm, which makes the possibility of these materials to be used as dopants in OLEDs using PVK as host. Moreover, the diphenylamino end-capped silafluorenes exhibited superior properties in device performance to those of carbazolyl end-capped ones in efficiencies and spectra stabilities. To further explore the utilities of the molecules, doped double-layer and triple-layer electroluminescent devices (as shown in Scheme 2) have been fabricated with configuration of ITO/PEDOT:PSS(40nm)/PVK:X(80nm)/Ca/Al, ITO/PEDOT:PSS(40nm)/PVK:X(80nm)/SPPO13(30nm)/Ca/Al, ITO/PEDOT:PSS(40nm)/PVK:OXD-7:X(80nm)/SPPO13(30nm)/Ca/Al, where X = **TDMS**, **TDPS**, or **DPFL-NPB**.

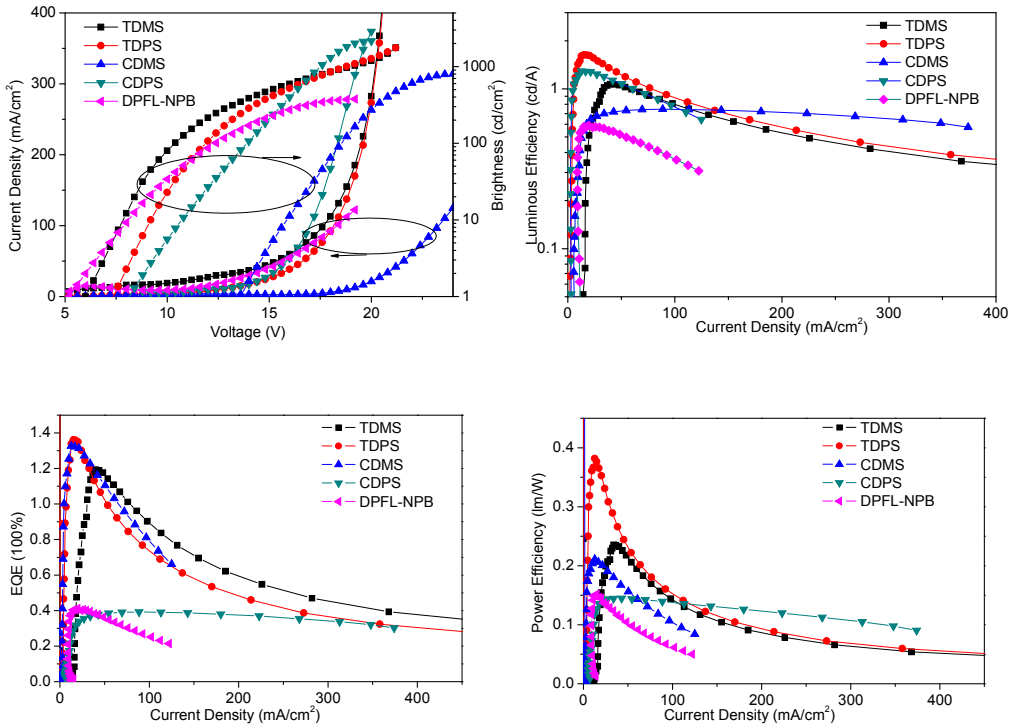

Fig. 4 Current-voltage-brightness, luminance-current density, external quantum efficiency-current density, and power efficiency-current density curves of **TDMS**, **TDPS**, **CDMS**, **CDPS** and **DPFL-NPB.**

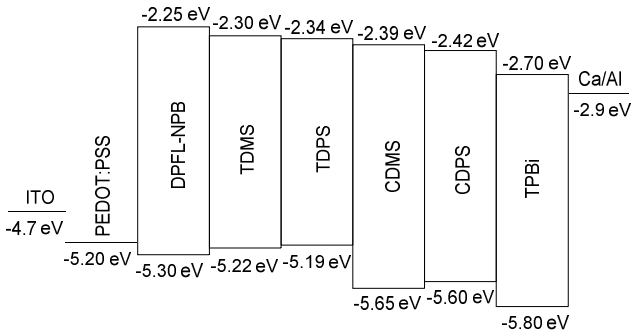

Fig. 5 Energy levels of emitters and the transporting-layer materials in device A.

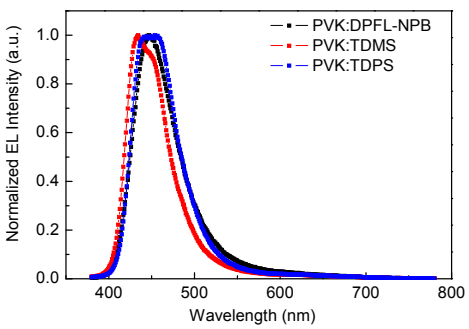

Fig. 6 EL spectra of device C with **TDMS**, **TDPS**, or **DPFL-NPB** as dopants.

Table 4 Summary of EL device performance of silafluorene derivatives based on device C

Device	V_{on}[a] (V)	V_{20}[b] (V)	$\eta_{l,20}$[c] (cd/A)	$\eta_{l,max}$[d] (cd/A)	$\eta_{p,20}$[e] (lm/W)	$\eta_{p,max}$[f] (lm/W)	L_{20}[g] (cd/m²)	L_{max}[h] (cd/m²)	EQE[i] (%)	λ_{EL}(fwhm)[j] (nm)
TDMS	8.0	14.4	1.23	1.28	0.68	0.68	256	1050	1.95	434(54)
TDPS	8.8	16.0	1.65	1.71	0.91	0.91	352	1674	2.12	454(61)
DPFL-NPB	7.6	13.6	1.19	1.22	0.34	0.34	239	1343	1.31	447(59)

[a]Turn on voltage when a brightness of 1 cd/m² observed. [b]Voltage taken at a current density of 20 mA/cm². [c]Current efficiency at a current density of 20 mA/cm². [d]Maximun current efficiency [e]Power efficiency at a current density of 20 mA/cm². [f]Maximum power efficiency. [g]Luminance at a current density of 20 mA/cm². [h]Maximum Luminance [i]External quantum efficiency at a current density of 20 mA/cm². [j]Full-width at half-maximum.

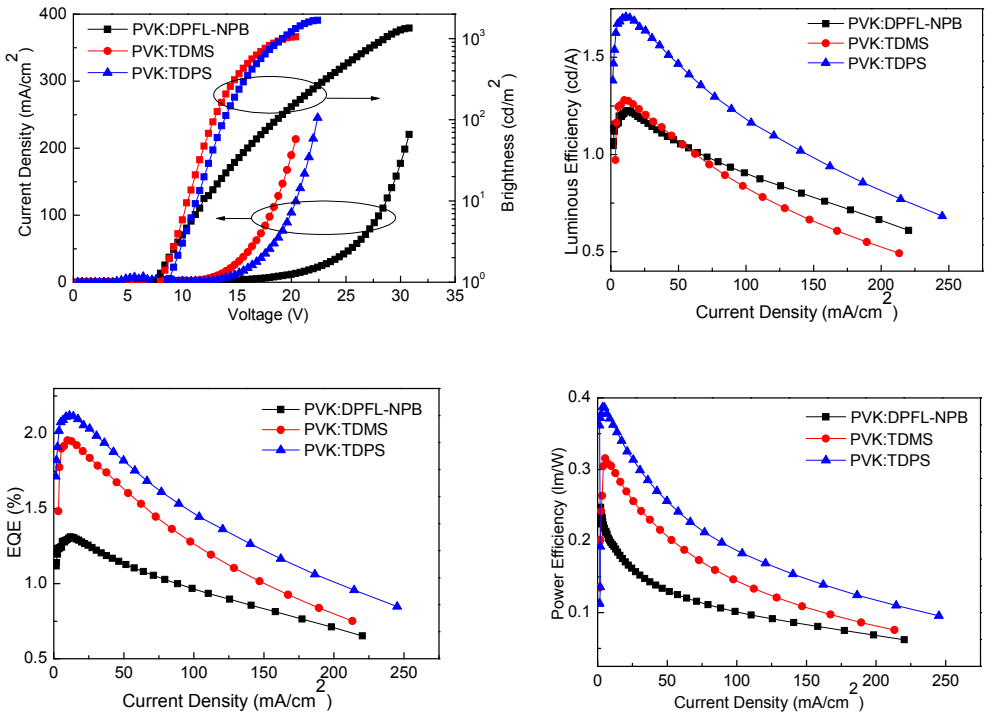

Fig. 7 Current-voltage-brightness, luminance-current density, external quantum efficiency-current density, and power efficiency-current density curves of device C with **TDMS**, **TDPS**, and **DPFL-NPB.**

PVK was used as host, while **TDMS**, **TDPS**, and **DPFL-NPB** were used as dopants. SPPO13 (2,7-bis(diphenylphosphoryl)-9,9-bispirobifluorene) was used as electron-transporting/hole-blocking material and OXD-7 (1,3-bis(2-(4-tert-butylphenyl)-1,3,4-oxadiazo-5-yl)benzene) was blended into the host matrix to facilitate the electron transport. Poly (3,4-ethylene dioxythiophene) : poly(styrenesulfonate) (PEDOT:PSS) was used as hole-injection layer. EL performances of device B indicated that the efficiencies of device with **TDPS** increase with the increase of **TDPS** percentage in the emitting-layer (EML) and the efficiencies are comparable to those of the reference material **DPFL-NPB** when a 100:20 ratio of PVK: **TDPS** is used (Table S1 and Figure S2, ESI†). However, the efficiencies of devices with **TDMS** are obviously lower than those of the references. Based on device B at the 100:20 ratio of host to dopant, an electron-transporting/hole-blocking layer of SPPO13 was introduced into device C, the efficiencies of both devices with **TDPS** and **TDMS** exhibited significant improvement as compared to those in device B and there was no long wavelength emission observed in the spectra with narrow FWHMs, which may derive from the improvement of charge balance in device C (Figure 6 and table 4). Detailed EL performances of all devices are summarized in Table 4 and Figure 7. Amongst the three devices, device with **TDPS** as dopant showed the best EL efficiencies with a maximum luminance of 1674cd/m^2, an external quantum yield of 2.12%, and a maximum luminous efficiency of 1.71cd/A, despite of a slightly high turn-on voltage compared with devices using **TDMS** and **DPFL-NPB**. To further improve the charge balance and excition confinement of the device, OXD-7 was blended into the host matrix in the ratio of PVK:OXD-7:X = 3:2:1 and the EL efficiencies of both devices with **TDMS** and **TDPS** were enhanced obviously (Table S2, Figure S3, and Figure S4, ESI†). The best device with **TDPS** exhibited a maximum luminance of 5501cd/m^2, an external quantum yield of 2.48%, a maximum luminous efficiency of 2.81cd/A, and a low turn-on voltage of 4V. However, all the spectra showed larger FWHMs as compared to those in the device C. All these results indicate that EL properties of these molecules could be modified by the 9-position substituents and the end-capped arylamino moieties and that these materials could be served as blue emitters.

Conclusions

In summary, a new homologous series of diphenylamino or cabazolyl end-capped silafluorenes for efficient blue-light emission of non-doped and doped double-layer EL devices have been synthesized and investigated. This class of materials show better promising OLED efficiencies than the commercially used reference **DPFL-NPB** in the non-doped double-layer devices. The device of ITO/**TDPS** (50nm)/TPBi(20nm)/Ca/Al gives the best performances in this series and exhibits a maximum current efficiency of 1.61 cd/A, a maximum brightness of 1794 cd/m^2, and an external quantum efficiency (EQE) of 1.36% with CIE coordinates of (0.175, 0.144) in deep to deep-blue region. The EL performances of the doped multi-layer devices with both **TDMS** and **TDPS** could be improved significantly by adding an electron-transporting/hole-blocking layer. In the device of ITO/PEDOT:PSS(40nm)/PVK:**TDPS**(80nm)/SPPO13(30nm)/Ca/Al, **TDPS** shows promising properties as doping material with

superior efficiencies to those of the commercially used material **DPFL-NPB**. Moreover, the devices using **TDPS** show better performances than those with the other materials in general. Further improvement could be achieved by adding the electon-transporting materials in the doped emitting-layer for charge banlance and excition confinement. These results indicate that the silafluorene end-capped with diphenylamino group show better electroluminescent efficiencies and stabilities and that introduction of diphenyl groups on 9-position could improve the material properties in OLEDs. Our findings show that these silafluorene derivatives could serve as efficient blue emitters for OLED applications and the properties of the derivatives could be tailored by changing the end-capped groups or the 9-position substituents in the silafluorene unit.

Experimental

Measurements

^{1}H and ^{13}C NMR spectra were recorded on a Bruker AM 400 spectrometer. Mass spectrometric measurements were recorded by a HP5989 mass spectrometer. UV-vis spectra were obtained on a Varian Cary 200 spectrophotometer. Fluorescence spectra were obtained on a Perkin-Elmer LS55 luminescence spectrometer. The differential scanning calorimetry (DSC) analysis was performed under a nitrogen atmosphere on a TA Instruments DSC 2920. Thermogravimetric analysis was undertaken using a TGA instrument (PE-TGA6). To measure the fluorescence quantum yields (Φ_F), degassed solutions of the compounds in different solvents were prepared and quinine sulfate monohydrate (Φ_{350} = 0.58 or Φ_{313} = 0.48) was used as a standard [39-40], while the absolute quantum yields Φ_F of the dyes in powder were measured by Edinburgh Photonics FLS920 fluorescence spectrometer. Fluorescence quantum yields in solution were calculated by equation 2 [41-42], where Φ_F, I_X, A_X, and n_X are quantum yield, fluorescence intensity, absorbance and refractive index of the measured solution and Φ_S, I_S, A_S, and n_S are the corresponding ones for the standard. Solution concentration was adjusted so that the absorbance of the solution would be lower than 0.1. Cyclic voltammetric (CV) measurements were carried out in a conventional three-electrode cell, using a Pt button working electrode 2 mm in diameter, a platinum wire counter electrode, and a $Ag/AgNO_3$ reference electrode on a computer-controlled EG&G Potentiostat/Galvanostat model 283 at room temperature. Reduction CV of all compounds was performed in dichloromethane containing Bu_4NPF_6 (0.1 M) as the supporting electrolyte.

$$\Phi_x = \Phi_s * \frac{I_x}{I_s} * \frac{A_s}{A_x} * \left(\frac{n_x}{n_s}\right)^2 \quad (2)$$

Device fabrication

The ITO-coated glass substrates were cleaned by detergent, ultra-sonicated in distilled water, acetone and alcohol sequentially and then treated with ultraviolet-ozone (UVO). For device A, the emitting layer and hole injection/transporting layer were fabricated onto the pretreated ITO glass in sequence under vacuum. For device B, C and D, a layer of 40 nm PEDOT:PSS was spin-coated onto the pretreated ITO substrates, annealed at 150 °C for 15 min, and then followed by an 80 nm emitting layer, annealed at 120 °C for 10 min in a nitrogen filled glove box (H_2O < 0.1 ppm, O_2< 0.1 ppm). For device C and D, SPPO13 was spin-coated after the emitting-layer and annealed at 80 °C for 20 min in a nitrogen filled glove box. Finally, Ca (10 nm)/Al (80 nm) was deposited onto the electron-transporting layer as a cathode by thermal evaporation under a vacuum of 3×10^{-6} Torr. The current density–luminance–voltage (*J–L–V*) and luminous efficiency–current density (η–*J*) characteristics were measured using a Keithley 2612B source-measurenment unit and a silicon photodiode that is calibrated by a PR-655 SpectraScan spectrophotometer. Electroluminescent (EL) spectra were recorded on a Maya 2000Pro spectrophotometer (Ocean Optics). CIE coordinates were calculated from the EL spectra.

Acknowledgments

We acknowledge Zhejiang Provincial Natural Science Foundation of China (ZJNSF LY13E030005) for financial support for this work.

Notes and references

[a] *Key Laboratory of Organosilicon Chemistry and Material Technology of Ministry of Education, Hangzhou Normal University, Hangzhou 310012, P. R. China. Fax: (+86)-571-28862271; E-mail:* xjfeng@hznu.edu.cn
[b] *School of Materials Science and Engineering, University of Science and Technology Beijing, Beijing 100083, P. R. China. E-mail:* xuxj@mater.ustb.edu.cn

† Electronic Supplementary Information (ESI) available: [synthesis and characterisation of the intermediates and final products, CV voltammograms, ELperformances of device B and device D]. See DOI: 10.1039/b000000x/

1 C.W. Tang and S.A. Van Slyke, *Appl. Phys. Lett.*, 1987, **51**, 913.
2 L.S. Huang and C.H. Chen, *Mater. Sci. Eng. R.*, 2002, **39**, 143.
3 F.-C. Chen, T. Yang, M.E. Thompson and J. Kido, *Appl. Phys. Lett.*, 2002, **80**, 2308.
4 B.W. D'Andrate and S.R. Forrest, *Adv. Mater.*, 2004, **16**, 1585,.
5 B. Chen, J. Ding, L. Wang, X. Jing and F. Wang, *Chem. Comm.*, 2012, **48** 8970.
6 M. Zhang, S.F. Xue, W.Y. Dong, Q. Wang, T. Fei, C. Gu and Y.G. Ma, *Chem. Commun.*, 2010, **46**, 3923.
7 D. Yokoyama, Y. Park, B. Kim, S. Kim, Y.-J. Pu, J. Kido and J. Park, *Appl. Phys. Lett.*, 2011, **99**, 123303.
8 I. Cho, S. H. Kim, J.H. Kim, S. Park and S.Y. Park, *J. Mater. Chem.*, 2012, **22**, 123.
9 H. Park, J. Lee, I. Kang, H.Y. Chu, J.-I. Lee, S.-K. Kwon and Y.-H. Kim, *J. Mater. Chem.*, 2012, **22**, 2695.
10 T.-C. Tsai, W.-Y. Hung, L.-C. Chi, K.-T. Wong, C.-C. Hsieh and P.-T. Chou, *Org. Electron.*, 2009, **10**, 158.
11 Y. Yang, P. Cohn, L. Dyer, S.-H. Eom, R. Reynolds, K. Castellano and J. Xue, *Chem. Mater.*, 2010, **22**, 3580.
12 L. Fisher, E. Linton, T. Kamtekar, C. Pearson, M.R. Bryce and M.C. Petty, *Chem. Mater.*, 2011, **23**, 1640.
13 Q.-X. Tong, S.-L. Lai, M.-Y. Chan, Y.-C. Zhou, H.-L. Kwong, C.-S. Lee, S.-T. Lee, T.-W. Lee, T. Noh and O. Keon, *J. Phys. Chem. C*, 2009, **113**, 6227.
14 K. He, X. Wang, J. Yu, H. Jiang, G. Xie, H. Tan, Y. Liu, D. Ma, Y. Wang and W. Zhu, *Org. Electron.*, 2014, **15**, 2942.
15 M.-J. Kim, C.-W. Lee and M.-S. Gong, *Org. Electron.*, 2014, **15**, 2922.
16 H.H. Fong, A. Papadimitratos, J. Hwang, A. Kahn and G. Malliaras, *Adv. Funct. Mater.*, 2009, **19**, 304.
17 T.-C. Chao, Y.-T. Lin, C.-Y. Yang, T.S. Hung, H.-C. Chou, C.-C. Wu and K.-T. Wong, *Adv. Mater.*, 2005, **17**, 992.

18 S. W. Culligan, Y. Geng, S. H. Chen, K. Klubek, K. M. Vaeth and C. W. Tang, *Adv. Mater.*, 2003, **15**, 1176.

19 E. Mondal, W.-Y. Hung, H.-C. Dai and K.-T. Wong, *Adv. Funct. Mater.*, 2013, **23**, 3096.

20 E. Mondal, W.-Y. Hung, Y.-H. Chen, M.-H. Cheng and K.-T. Wong, *Chem. Eur. J.*, 2013, **19**, 10563.

21 S. Ye, J. Chen, C. Di, Y. Liu, K. Lu, W. Wu, C. Du, Y. Liu, Z. Shuai and G. Yu, *J. Mater. Chem.*, 2010, **20**, 3186.

22 C. Fan, Y. Chen, Z. Jiang, C. Yang, C. Zhong, J. Qin and D. Ma, *J. Mater. Chem.*, 2010, **20**, 3232.

23 U. Giovanella, C. Botta, F. Galeotti, B. Vercelli, S. Battiato and M. Pasini, *J. Mater. Chem. C*, 2013, **1**, 5322.

24 H. Liang, X. Wang, X. Zhang, Z. Liu, Z. Ge, X. Ouyang and S. Wang, *New J. Chem.*, 2014, **38**, 4696.

25 Y.-L. Liao, W.-Y. Hung, T.-H. Hou, C.-Y. Lin and K.-T. Wong, *Chem. Mater.*, 2007, **19**, 6350.

26 G. Klaerner, M. H. Davey, W. D. Chen, J. C. Scott and R. D. Miller, *Adv. Mater.*, 1998, **10**, 993.

27 X. Gong, P. K. Iyer, G. C. Bazan, A. J. Heeger and S. S. Xiao, *Adv. Funct.Mater.*, 2003, **13**, 325.

28 K.L. Chan, J. McKiernan, R. Towns and B. Holmes, *J. Am. Chem. Soc.*, 2005, **127**, 7662.

29 E. Wang, C. Li, W. Zhuang, J. Peng and Y. Cao, *J. Mater. Chem.*, 2008, **18**, 797.

30 A.L. Fisher, K. E. Linton, K.T. Kamtekar, C. Pearson, M.R. Bryce and M. C. Petty, *Chem. Mater.*, 2011, **23**, 1640.

31 S. Oyston, C. Wang, G. Hughes, A.S. Batsanov, I.F. Perepichka, M.R. Bryce, J.H. Ahn, C. Pearson and M.C. Petty, *J. Mater. Chem.*, 2005, **15**, 194.

32 C. Pearson, J.H. Ahn, M.F. Mabrook, D.A. Zeze, M.C. Petty, K.T. Kamtekar, C. Wang, M.R. Bryce, P. Dimitrakis and D.Tsoukalas, *Appl. Phys. Lett.*, 2007, **91**, 123506.

33 K.E. Linton, A.L. Fisher, C. Pearson, M.A. Fox, L.-O. Palsson, M.R. Bryce and M.C. Petty, *J. Mater. Chem.*, 2012, **22**, 11816.

34 X.J. Feng, S.F. Chen, Y. Ni, M.S. Wong, M.K. Lam, K.W. Cheah and G.Q. Lai, *Org. Electron.*, 2014, **15**, 57.

35 K.L. Chan, M.J. McKiernan, C.R. Towns and A.B. Holmes, *J. Am. Chem. Soc.*, 2005, **127**, 7662.

36 B.-S. Kim, S.-H. Kim, Y.-S. Kim, S.-H. Kim and Y.-A. Son, *Mol. Cryst. Liq. Cryst.*, 2009, **504**, 173.

37 F. Polo, F. Rizzo, M. Veiga-Gutierrez, L. D. Cola and S Quici, *J. Am. Chem. Soc.*, 2012, **134**, 15402.

38 M.J. Frisch, G.W. Trucks, H.B. Schlegel, G.E. Scuseria, M.A. Robb, J.R. Cheeseman, G. Scalmani, V. Barone, B. Mennucci, G.A. Petersson, H. Nakatsuji, M. Caricato, X. Li, H.P. Hratchian, A.F. Izmaylov, J. Bloino, G. Zheng, J.L. Sonnenberg, M. Hada, M. Ehara, K. Toyota, R. Fukuda, J. Hasegawa, M. Ishida, T. Nakajima, Y. Honda, O. Kitao, H. Nakai, T. Vreven, J.A. Montgomery, Jr., J.E. Peralta, F. Ogliaro, M. Bearpark, J.J. Heyd, E. Brothers, K.N. Kudin, V.N. Staroverov, T. Keith, R. Kobayashi, J. Normand, K. Raghavachari, A. Rendell, J.C. Burant, S.S. Iyengar, J. Tomasi, M. Cossi, N. Rega, J.M. Millam, M. Klene, J.E. Knox, J.B. Cross, V. Bakken, C. Adamo, J. Jaramillo, R. Gomperts, R.E. Stratmann, O. Yazyev, A.J. Austin, R. Cammi, C. Pomelli, J.W. Ochterski, R.L. Martin, K. Morokuma, V.G. Zakrzewski, G.A. Voth, P. Salvador, J.J. Dannenberg, S. Dapprich, A.D. Daniels, O. Farkas, J.B. Foresman, J.V. Ortiz, J. Cioslowski and D.J. Fox, *Gaussian 09, Revision C.01*,Gaussian, Inc., Wallingford CT, **2010**.

39 J. E. Gill, *Photochem. Photobiol.,* 1969, **9**, 313.

40 W. R. Dawdon and M. W. Windsor, *J. Phys. Chem.,* 1968, **72**, 3251.

41 H. V. Drushel, A.L. Sommers and R. C. Cox, *Anal. Chem.*, 1963, **35**, 2166.

42 C. A. Parker and W. T. Rees, *Analyst*, 1960, **85**, 587.

Text:

Silafluorene derivatives are designed for blue OLEDs and tunable efficiencies are investigated by end-capped arylamino groups and subtituent groups on silicon atom.

Graphic: